A SAXS STUDY OF SILICA AEROGELS

A. CRAIEVICH

Centro Brasileiro de Pesquisas Físicas, Rua Xavier Sigaud 150, 22290 Rio de Janeiro, R.J., Brazil

M.A. AEGERTER and D.I. dos SANTOS

Istituto de Física e Química de São Carlos, University of São Paulo, Cx Postal 369, 13560 São Carlos, S.P., Brazil

T. WOIGNIER and J. ZARZYCKI

Laboratory of Science of Vitreous Materials, L.A. 1119, University of Montpellier, 34060 Montpellier Cedex, France

Received 4 April 1986

Aerogels produced by hypercritical drying of gels from hydrolysis of TMOS in various pH conditions and subjected to a densification process were studied by SAXS using the LURE synchrotron facility. The evaluation of scattering data combined with BET measurements leads to a model of aerogels consisting of a light density matrix in which meso- and macro-pores are embedded. No fractal features were observed for the gels, the Porod's limit having an exponent *n* = 4. This could mean that either these aerogels are not fractals or that the SAXS method suffers from an inherent ambiguity for fractal dimension *D* = 3.

1. Introduction

Recent renewed interest in silica aerogels is linked to the role played by these materials in the synthesis of glasses from gels.

To avoid cracking of gels during drying, which is due to the action of capillary forces, hypercritical evacuation can be advantageously used [1]. Monolithic aerogels produced in this way represent an intermediate stage in the synthesis of glasses by the gel route. As the subsequent curing and consolidation stages which lead to homogenisation depend closely on the initial texture of the material, structural characteristics of aerogels are of prime importance.

From a more fundamental standpoint it was claimed that some gels may be considered as fractal objects [2] and various physico-chemical methods are currently used to try to prove or disprove this point [3–6]. Small-angle scattering of X-rays (SAXS) is a choice method for studying the structure of materials in the 1–100 nm range; it was proposed as a tool for solving fractal features [7,8].

2. SAXS method

In order to determine structure-related geometrical parameters, one can start from the hypothesis that aerogels can be approximately described by a "two-electronic density" model in which ρ_e is the electronic density of the matrix and $\rho = 0$ corresponds to the empty (air-filled) pores.

If one of the phases occupies a low volume fraction, the structure can usually be described as a diluted system of "particles" which can be either material particles or voids. If the system is composed of identical particles (monodispersed) the intensity of X-rays scattered at low angles follows Guinier's law [9]:

$$I(q) = N\rho_e^2 v^2 \exp\left(-\tfrac{1}{3}R_G^2 q^2\right), \tag{1}$$

where $I(q)$ is the SAXS intensity at low angles as a function of the modulus of the scattering vector $q = 4\pi(\sin\theta)/\lambda$, 2θ being the scattering angle, λ the X-ray wavelength, N the number of particles (or voids) of volume v and R_G the (electronic) radius of gyration of the particles. R_G can be determined from SAXS measurements on a relative scale.

For a polydispersed system a weighted average radius of gyration $\langle R_G \rangle$ is obtained from the relation:

$$\langle R_G \rangle^2 = \sum_i R_i^2 v_i^2 p_i \Big/ \sum_i v_i^2 p_i, \tag{2}$$

where p_i is the fraction of particles of volume v_i with a gyration radius R_i; $\langle R_G \rangle$ is heavily weighted towards larger particles.

For non-diluted (dense) particle systems, Guinier's law is still approximately obeyed in a rather wide angular domain but the intensity curve may show a maximum. For such systems a value of R_G can also be determined from Eq. (1) but, in this case, it is an "apparent" radius of gyration, R_a, usually lower than that of the diluted system. The apparent radius of gyration is a geometrical parameter which may be useful to indicate, by comparison, variations or tendencies associated with the average sizes of the particles.

Other parameters can be determined from SAXS experiments on "two density" systems. For a system of two phases of volume fraction Φ and $1 - \Phi$ and if the measurements are made in relative units, a correlation volume V_c and the area of the interface between the two phases per unit volume S/V may be obtained from the following relations:

$$\frac{V_c}{2\pi^2} = \frac{I(0)}{Q_0} \tag{3}$$

and

$$\frac{1}{\pi\Phi(1-\Phi)}\left(\frac{S}{V}\right) = \frac{\displaystyle\lim_{q\to\infty}\left[I(q)q^4\right]}{Q_0}. \tag{4}$$

In these equations Q_0 is the "integrated intensity"

$$Q_0 = \int_0^\infty I(q) q^2 dq \qquad (5)$$

and $I(0)$ the extrapolated scattered intensity at zero angle, both of these measured on the same relative scale. For diluted systems V_c is an average particle volume. For dense systems of particles, V_c is a geometrical parameter which can be qualitatively associated with the average volume. This parameter is closer to the average volume when the volume fraction occupied by the particle tends to zero.

For a two-density system the expression $I(q)q^4$ tends, for high q-values, towards a constant P over a wide range of q:

$$\lim_{q\to\infty}\left[I(q)q^4\right] = P. \qquad (6)$$

This is Porod's law which holds if the interface is smooth. If the surface exhibits "fractal" features, the classical surface area has an ambiguous meaning. For this type of surfaces Porod's law becomes:

$$\lim_{q\to\infty}\left[I(q)q^{(6-D)}\right] = \text{constant}, \qquad (7)$$

where D is the dimensionality of the fractal surface. $D = 2$ corresponds to classical (two-dimensional) surfaces. Several humid gels were shown to exhibit interfaces having fractal properties with $2 < D < 3$ [10,11].

From Eq. (4), which is valid for any value of Φ, the specific interface S/V may be determined from SAXS experiments if Φ is known. Inversely, if S/V can be determined by an independent (e.g. BET) method, SAXS experiments permit to obtain the fraction Φ and the density of the scattering phases.

3. Preparation of the samples

Silica gels were prepared from solutions of tetramethoxysilane (TMOS) (FLUKA) dissolved in methanol; the composition varied between 20 and 70 vol% of TMOS. To these solutions 4 moles of bidistilled H_2O per mole of TMOS was added for all TMOS concentrations prepared.

The pH of water was modified by the addition of either 0.01 N HNO_3 or 0.01 N NH_4OH. After a few minutes of vigorous stirring, the solutions were transferred into pyrex tubes and maintained at 50°C until gelification was completed, which usually occurred in a few hours. The tubes were stored at this temperature until the wet gel separated from the walls allowing to remove them without breaking.

The gels were then dried hypercritically in an autoclave with an equipment and procedure similar to that previously described [12]. The amount of methanol added permitted to reach a pressure of about 160 bar at 300°C. The rate of heating was about 4°C/min.

The aerogel rods obtained in this way were typically 1.5 cm in diameter and 17 cm in length. From these rods disks of a few millimetres thickness were cut using a high-precision (Meyer Burger) diamond saw.

Some of the samples were thermally treated at 1080°C in air for varying lengths of time to density them. The apparent density, d, of the sample was measured with a mercury volumeter or by determining the ratio of the aerogel weight to its geometrical volume.

The BET specific surface S' of the samples was determined on particles of a few mm^3 volume using a Micromeritics 2100 equipment.

The thickness, t, of the samples used in the SAXS experiments was close to the optimum value $t_m = 1/d\mu$ where μ is the X-ray absorption factor and d the apparent density. t_m was 0.2 to 1 mm depending on the density of the sample. The surfaces of untreated samples were as received from diamond saw cutting. The densified samples were polished on both faces.

4. Experimental

The SAXS experiments were carried out using synchrotron radiation at LURE (Orsay, France). The X-ray source (DCI positron storage ring) with an appropriated collimation provides a very intense monochromatic beam with point-like cross-section. This type of collimation allowed SAXS data to be obtained from the aerogels in a short time and without the necessity of mathematical desmearing (for slit height and width). This is essential to improve the accuracy of the experimental results in order to test possible fractal behaviour.

The white beam from the storage ring is monochromatized by a double-crystal monochromator of Si tuned for 8 keV ($\lambda = 1.55$ Å). Two sets of slits define the beam cross-section and diminish the parasitic scattering. A one-dimensional position-sensitive detector was used to record the scattered X-ray intensity from the plate-shaped aerogel samples.

The parasitic scattering from air and slits was subtracted from the experimental SAXS intensity using standard methods. All SAXS curves were determined on a relative scale.

5. Results

The experimental results were classified into three groups which correspond to: (a) aerogels prepared from neutral solutions of different TMOS content; (b) aerogels of 50% TMOS content produced under different pH conditions; and (c) neutral aerogels with 50% TMOS content heat-treated at 1080°C for increasing lengths of time.

Figs. 1(a, b, c) show as an example the experimental SAXS curves of group (b) which correspond

(A) and basic (B) solutions. All these curves, as well as those of groups (a) and (c), exhibit maxima on the low-angle side. Such maxima are generally observed for very dense particle systems and correspond to strong deviations from Guinier's law at very small scattering angles.

Figs. 2(a, b and c) correspond respectively to the three groups defined above; they were plotted in log $I(q)$ versus log q scale in order to detect eventual fractal behaviour. It can be seen that every plot is nonlinear within the whole q domain. This implies that neither Eq. (6) nor (7) apply. Then these equations may correspond to asymptotic behaviours which are obviously not verified for the aerogels in the q domain comprised between 0.005 Å⁻¹ and 0.06 Å⁻¹. Therefore additional SAXS experiments were carried out, placing the position-sensitive detector at a shorter distance from the sample. These new SAXS curves are shown in figs. 3(a, b, c), in log $I(q)$ versus log q scale, for the extended q range 0.06 Å⁻¹ to 0.25 Å⁻¹. They complete figs. 2(a, b and c) respectively.

It can be seen that all the SAXS plots of figs. 3 tend towards a linear behaviour indicated by the dashed straight lines with a slope equal to −4. This seems to prove that Porod's law is obeyed in each case when the range of
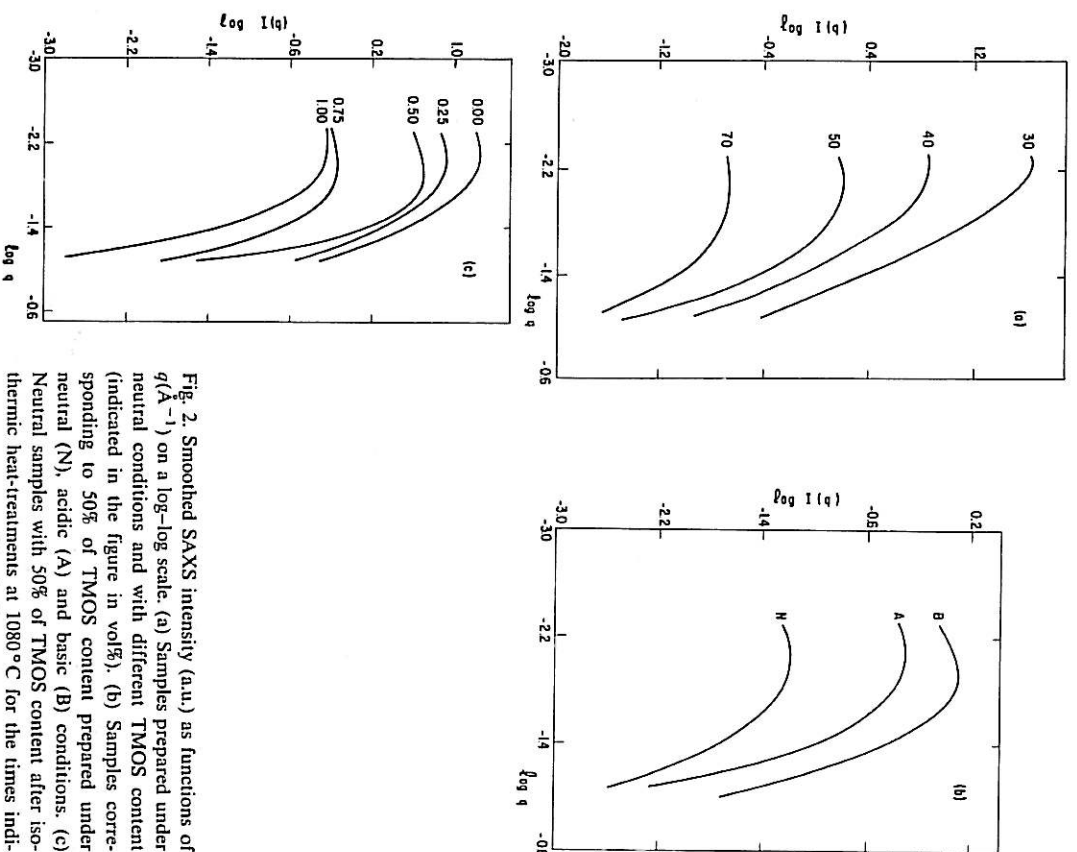
Fig. 1. Smoothed SAXS intensities as functions of the modulus of the scattering vector corresponding to aerogels prepared from solutions containing 50 vol% of TMOS under different conditions: (a) neutral, (b) acid, (c) basic.

q is sufficiently extended. The slope −4 implies the absence of fractal features for the interface surfaces and allows Eq. (4) to be used to estimate the specific area of the (smooth) interfaces.

The SAXS curves were also plotted on a log $I(q)$ versus q^2 scale, in order to verify, the extent of validity of Guinier's law (Eq. (1)). These plots are presented in figs. 4(a, b and c) for sample groups (a), (b) and (c) respectively. Linear regions within a more or less extended a domain, depending on the

Fig. 2. Smoothed SAXS intensity (a.u.) as functions of $q(\text{Å}^{-1})$ on a log–log scale. (a) Samples prepared under neutral conditions and with different TMOS content (indicated in the figure in vol%). (b) Samples corresponding to 50% of TMOS content prepared under neutral (N), acidic (A) and basic (B) conditions. (c) Neutral samples with 50% of TMOS content after isothermic heat-treatments at 1080°C for the times indicated in the figure (hours).
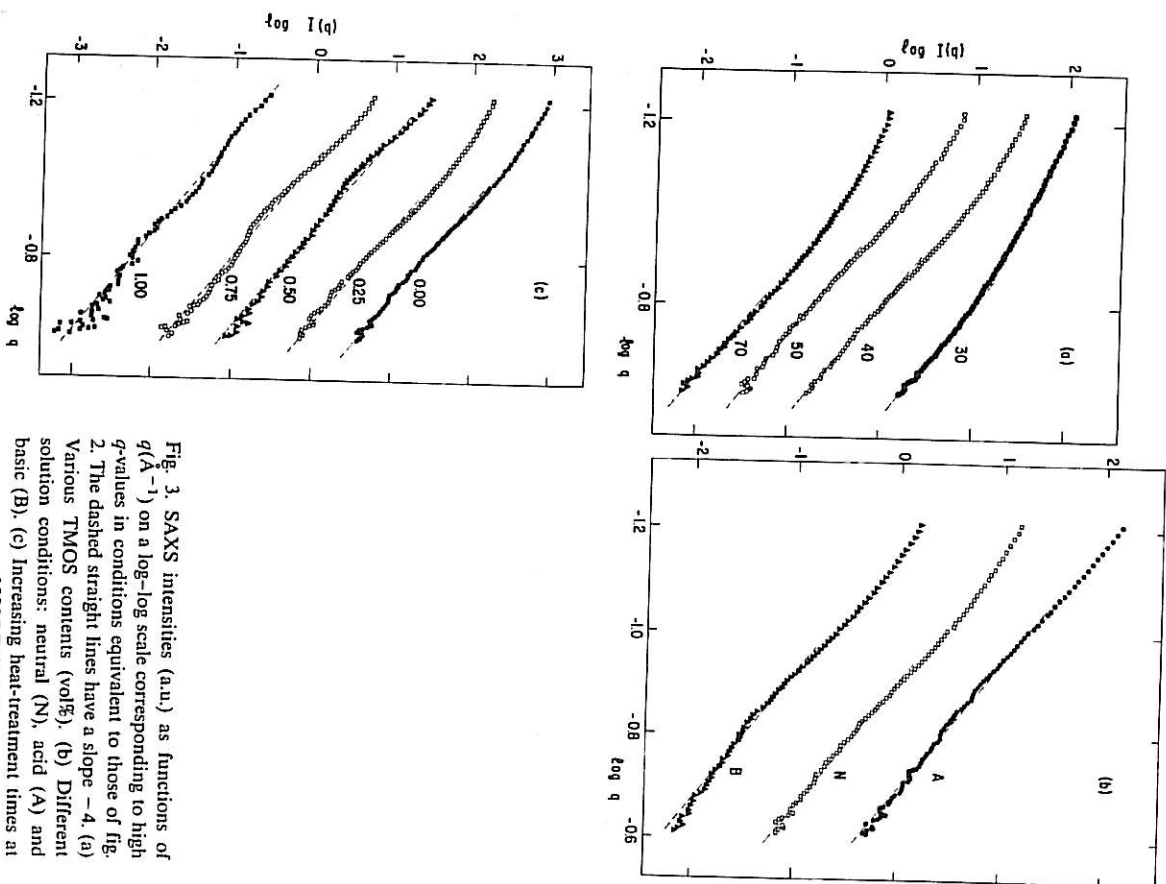
Fig. 3. SAXS intensities (a.u.) as functions of $q(\text{Å}^{-1})$ on a log-log scale corresponding to high q-values in conditions equivalent to those of fig. 2. The dashed straight lines have a slope −4. (a) Various TMOS contents (vol%). (b) Different solution conditions: neutral (N), acid (A) and basic (B). (c) Increasing heat-treatment times at 1080°C (hours).

sample, can be observed in every plot of figs. 4(a, b and c). The linear portions of these plots were used to calculate the apparent average radius of gyration R_a of the "particles" in every sample. The values of R_a are assembled in table 1 (a, b, c). For one of the aerogels of group (c) ($d = 1.16$ g/cm³) two values of
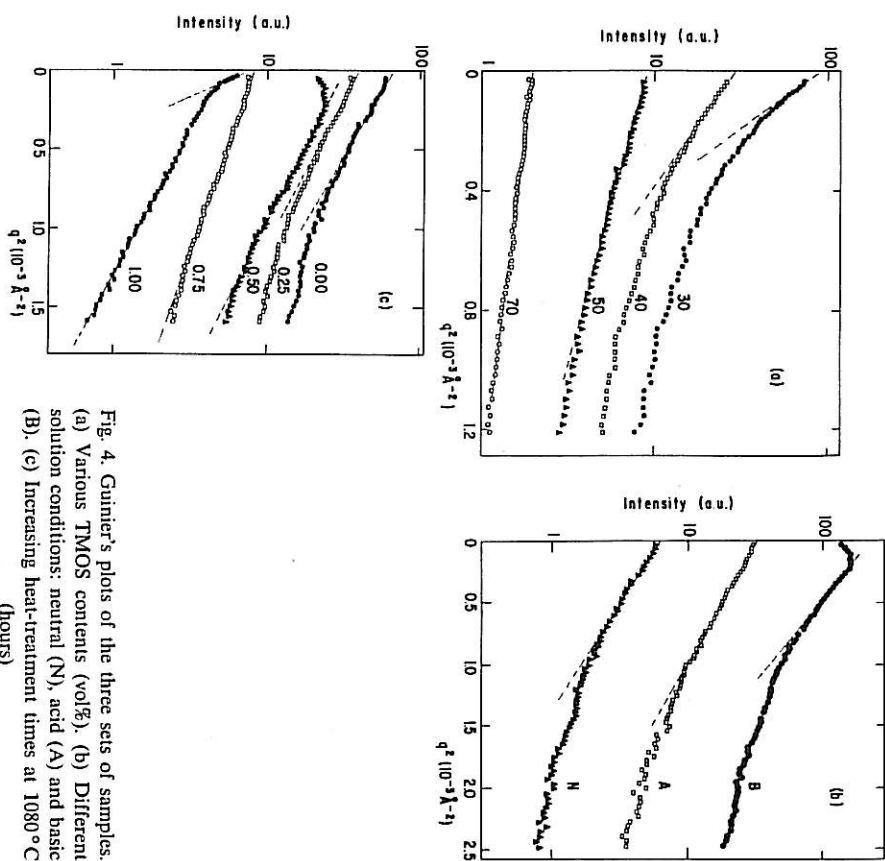
Fig 4. Guinier's plots of the three sets of samples. (a) Various TMOS contents (vol%). (b) Different solution conditions: neutral (N), acid (A) and basic (B). (c) Increasing heat-treatment times at 1080°C (hours)

R_a were obtained which correspond to the two slopes of the straight lines in the plot of fig. 4(c). This suggests a particle size distribution of bimodal type for this particular aerogel.

The integrated intensity Q_0 was determined by numerical integration of the scattered intensity. $I(0)$ and P were estimated from the curves of figs. 4. Using these values and Eqs. (3) and (4) the values of V_c and $(S/V)\Phi(1-\Phi)$ were obtained. They are shown in table 1, together with the value of the surface area of the interface per unit mass $S' = S/Vd$ and $(S/V)\Phi(1-\Phi)$ determined by BET.

From these values the parameter $K = \Phi(1-\Phi)$ was obtained which fixes the fractions of the two coexisting phases:

$$\Phi = \frac{1 \pm (1-4K)^{1/2}}{2}$$

Table 1

(a) Neutral gels, influence of TMOS (%)

TMOS (vol%)	d (g/cm³)	S' (m²/g)	V_c (10⁶Å³)	R_a (Å)	R'_a (Å)	$(S/V)/\Phi(1-\Phi)$ (m²/cm³)
30	0.23	656	1.01	90	48	1128
40	0.29	383	0.632	64	41	939
50	0.35	339	0.348	40	34	895
70	0.52	496	0.151	27	25.5	1137

(b) Influence of conditions of catalysis

Catalysis	d (g/cm³)	S' (m²/g)	V_c (10⁶Å³)	R_a (Å)	R'_a (Å)	$(S/V)/\Phi(1-\Phi)$ (m²/cm³)
B	0.16	426	0.337	46	33	792
A	0.41	277	0.475	38	37	644
N	0.35	339	0.348	40	34	895

(c) Sintering behaviour

Time at 1080° (h)	d (g/cm³)	S' (m²/g)	V_c (10⁶Å³)	R_a (Å)	R'_a (Å)	$(S/V)/\Phi(1-\Phi)$ (m²/cm³)
0	0.35		0.348	40	39	895
0.25	0.39		0.304	39	32	958
0.50	0.45		0.511	39	38	352
0.75	0.82		0.357	32	34	631
1.00	1.16		1.137	40–78	50	377

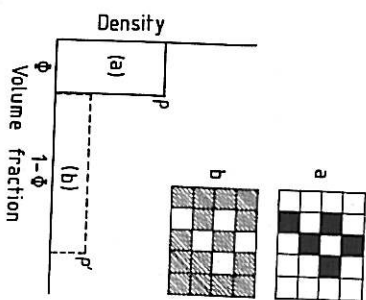S' was not determined in (c).

Fig. 5. Models of scattering "particles" (schematic): (a) dense particles (ρ); (b) pores in a low-density matrix (ρ'). The models have the same apparent density and interface.
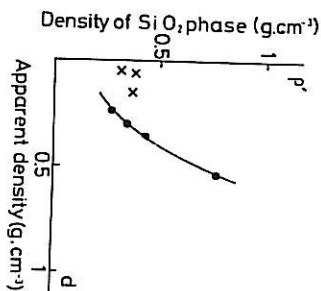

Fig. 6. Matrix density ρ' versus apparent density d of SiO₂ aerogels with different TMOS %: x: results of Mulder et al. [13].

Table 2

(a) Density calculation for neutral aerogels with different TMOS %

TMOS (%)	K	Φ	$1-\Phi$	ρ (g/cm³)	ρ' (g/cm³)
30	0.134	0.158	0.842	1.455	0.273
40	0.118	0.137	0.863	2.197	0.334
50	0.133	0.158	0.842	2.21	0.415
70	0.227	0.348	0.652	1.49	0.798

(b) Density calculation for 50% TMOS aerogels according to the type of catalysis

Type of catalysis	K	Φ	$1-\Phi$	ρ (g/cm³)	ρ' (g/cm³)
B	0.086	0.095	0.905	1.68	0.176
A	0.776	0.228	0.772	1.798	0.531
N	0.133	0.158	0.842	2.21	0.415

6. Discussion

The essential problem is the assignment of the respective densities to the coexisting phases which leaves two possibilities: (fig. 5a, b):

(a) The solid "particles" of the system form the fraction Φ of density ρ; the remaining fraction $1 - \Phi$ then corresponds to air-filled pores of zero density.

(b) The "particles" detected by scattering effects are pores occupying the fraction Φ, the remaining fraction $1 - \Phi$ of density ρ' corresponding to the solid matrix.

If the parameter $K \neq 0.25$ one can distinguish the major from the minor phase and $\rho \neq \rho'$. If d is the apparent density of the sample we have

$$\rho = d/\Phi \quad \text{and} \quad \rho' = d/(1 - \Phi).$$

Table 2 (a) shows the values of ρ and ρ' calculated from the preceding data for group (a). It can be seen that as $K < 0.25$ the concept of minor and major phases has a meaning and that ρ' values show a monotonic trend with % TMOS while ρ values vary irregularly. The surprisingly low values of ρ' are close to those recently estimated by Mulder et al. from electron microscopic observations [13]. Fig. 6 shows the evolution of ρ' as a function of the apparent density d.

6.1. Structural model

The model of the texture of these aerogels (fig. 7a) can be visualized as a sponge formed by a light matrix material containing essentially closed micropores in the 5–10 Å range, which reduce its apparent skeletal density to the small observed value ρ'
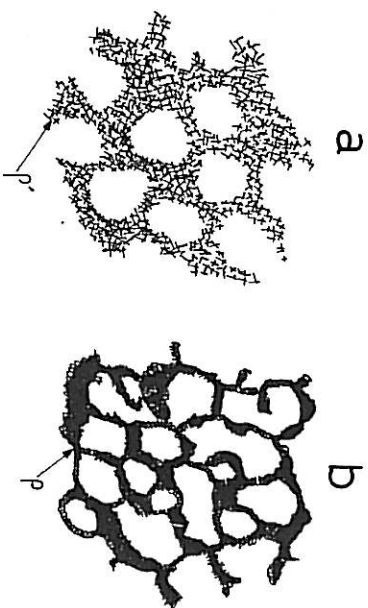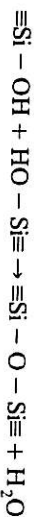
This matrix contains meso- and macro-pores which give rise to scattering effects observed in SAXS experiments and the surface of which is measured by BET.
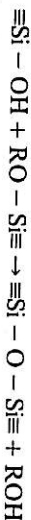
The evaluation of data of series (b) (table 2b) shows that, while for aerogels formed in neutral or acid conditions a model based on a light matrix ρ' seems correct, for gels formed in basic conditions a model with a higher density ($\rho = 1.68$) seems preferable (fig. 7b). This is consistent with the EM observations that basic gels are formed of particles which are almost fully polymerized and the skeletal density of which should approach more closely the density of solid silica: ($\rho_s = 2.2$ g/cm³).

6.2. Behaviour during sintering

During sintering, the micropores are first eliminated by polycondensation reactions of the type

$$\equiv Si - OH + RO - Si \equiv \rightarrow \equiv Si - O - Si \equiv + ROH$$

or

$$\equiv Si - OH + HO - Si \equiv \rightarrow \equiv Si - O - Si \equiv + H_2O$$

This corresponds to the first stage of sintering dominated by the diffusion mechanism [14] and should result in a progressive increase in the matrix density ρ'. In a second phase, meso- and macro-pores would be eliminated by coalescence and densification by viscous flow.

It is interesting to follow the trends shown by the "geometrical" parameters R_a and V_c. In order to have comparable parameters a correlation gyration radius R'_a was obtained from V_c assuming the volume V_c spherical. R_a and R'_a are used to characterize the size of meso- and macro-pores.

The data for the three groups of samples corresponding to (a) influence of

Fig. 7. Models of aerogels: (a) acid- and (b) base-catalysed.

TMOS, (b) conditions of catalysis, and (c) sintering behaviour, are contained in tables 1(a, b, c).

Table 1(a) shows that both R_a and R'_a decrease regularly and become closer when the TMOS concentration increases. This trend means that the size of the mesopores decreases and that they become more spherical when the density increases.

Table 1(b) shows that, according to pH, mesopores are roughly of similar size but that their shape is more regular for acid gels than for basic ones (R_a closer to R'_a).

Table 1(c) shows that for $0.35 < d < 0.82$ R_a decreases while R'_a is rather stable. This could correspond to a spherodization of pores during sintering combined with a coalescence effect leading to a bimodal distribution for $d = 1.16$.

6.3. Fractal features

The rather surprising fact that Porod's law is obeyed in all cases ($I(q) \cdot q^n$ = constant, with $n = 4$) means that the fractal dimension is $D = 2$, i.e. that these aerogels are indeed not fractals at all. It is possible that the texture of these aerogels does not fulfil the self-similarity conditions required in fractal objects.

It is also possible that the SAXS method suffers from an inherent ambiguity. It has been claimed recently [15] that Eq. (7) should only be applicable to cases with $2 < D < 3$ and that for the limiting value $D = 3$ and $D = 2$ the relation reduces to Porod's law. If this is true, SAXS method would be incapable of distinguishing between a classic (smooth) interface and a fractal surface with $D = 3$. This point will be studied in more detail.

7. Conclusion

High-precision small-angle X-ray diffraction spectra of aerogels were obtained using a synchrotron radiation facility. The results combined with BET measurements lead to a textural model which consists of an extremely light matrix (~ 0.3–0.4 g/cm³) containing large air-filled meso- and macro-pores which produce the scattering observed.

Surprisingly, all experiments show that Porod's law limit is closely obeyed. This means that either these aerogels are not fractals or that the SAXS method itself suffers from an inherent ambiguity for the limiting fractal dimension $D = 3$.

References

[1] J. Zarzycki, in: Glass: Science and Technology, Vol 2, Eds. D.R. Uhlmann and N.J. Kreidl (Academic Press, New York, 1984) pp. 209–249.

[2] D. Avnir, D. Farin and P. Pfeifer, Nature 308 (1984) 261.

[3] P. Pfeifer and D. Avnir, J. Chem. Phys. 79 (1983) 3558.

[4] D. Avnir, D. Farin and P. Pfeifer, J. Chem. Phys. 79 (1983) 3566.

[5] D. Avnir and P. Pfeifer, Nouv. J. Chem. 7 (1983) 71.

[6] U. Even, K. Rademann, J. Jortner, N. Manor and R. Reisfeld, Phys. Rev. Lett. 52 (1984) 2164.

[7] H.D. Bale and P.W. Schmidt, Phys. Rev. Lett. 53 (1984) 596.

[8] D.W. Schaefer and K.D. Keefer, Phys. Rev. Lett. 53 (1984) 1383.

[9] O. Glatter, and O. Kratky, Small Angle X-ray Scattering (Academic Press, New York, 1982).

[10] D.W. Schaefer and K.D. Keefer, in: Better Ceramics Through Chemistry Eds. J. Brinker, D. Clark, D. Ulrich (Elsevier, New York, 1984) p. 1.

[11] K.D. Keefer, in Ref. [10], p. 15.

[12] J. Zarzycki, M. Prassas and J. Phalippou, J. Mater. Sci. 17 (1982) 3371.

[13] C.A.M. Mulder, G. Van Leeuwen, J.G. Van Lierop and J.P. Woerdman, 3rd Int. Workshop on Glasses and Glass-Cermics from Gels, Montpellier (Sept. 12–14, 1985) J. Non-Cryst. Solids 82 (1986) 148.

[14] M. Prassas, J. Phalippou and J. Zarzycki, 2nd Int. Conf. on Ultrastructure Processing of Ceramics, Glasses and Composites, Palm Coast, FL (Feb. 25–March 1, 1985).

[15] D. Rojanski, D. Huppert, H.B. Bale, X. Dacai, P.W. Schmidt, D. Farin, A. Seri-Levy and D. Avnir, Proc. 2nd Int. Conf. Unconventional Photoactive Materials, Cleveland, OH (Sept. 1986) Ed. H. Scher (Plenum, New York, 1986).